AAPS PharmSciTech (2025) 26:145
https://doi.org/10.1208/s12249-025-03133-4

RESEARCH ARTICLE

Mitigating Shear Stress in Spray Drying for RNA-Loaded Lipid Nanoparticles through Process and Formulation Optimization

Susana Farinha[1,2,3] · Rute Mota[1,2,4,5] · Carolina Lopes[1] · Ricardo Velez[1] · Mara G. Freire[4] · Ana Aguiar-Ricardo[5] · Miguel Ângelo Rodrigues[3] · Luís Marques[1] · Joana S. Cristóvão[2] · Paulo Roque Lino[1]

Received: 17 December 2024 / Accepted: 28 April 2025

Abstract

Lipid nanoparticles (LNPs) have emerged as effective delivery systems for nucleic acid therapies, exemplified by the success of Moderna and Pfizer/BioNTech COVID-19 vaccines. However, these therapies still present significant shelf-life stability limitations, often requiring conservative cold chain storage conditions. Given the hurdles associated with cold chain supply, it is critical to overcome the stability challenges of these therapies. Drying technologies, such as spray drying (SD), can improve stability by removing water and preventing RNA hydrolysis and degradation. Nonetheless, shear and thermal stresses from SD can introduce additional risks to both the nucleic acid and the delivery system. Here, microfluidics was used to produce ribonucleic acid (RNA)-loaded LNPs with high encapsulation efficiency (> 95%), which were subsequently used to optimize the SD. A thorough process and formulation optimization was performed to maintain the LNPs' colloidal stability and nucleic acid encapsulation efficiency after spray drying. Poloxamer 188 (P188) proved crucial in protecting LNPs from shear stress possibly due to its ability to insert itself within lipid layers, allowing the maintenance of colloidal stability during SD. Additionally, SD was benchmarked against freeze drying (FD) as an alternative low shear drying technology. Overall, the study demonstrates the importance of optimizing the SD process to enhance nucleic acid-loaded LNPs' stability and delivery potential.

Susana Farinha and Rute Mota contributed equally to this work.

✉ Paulo Roque Lino
plino@hovione.com

1 R&D Inhalation and Advanced Drug Delivery, Hovione Farmaciência S.A, Estrada Do Lumiar, Campus Do Lumiar, Edifício R, Lisbon 1649-038, Portugal

2 Hovione Farmaciência S.A, R&D Analytical Development, Estrada Do Lumiar, Campus Do Lumiar, Edifício R, Lisbon 1649-038, Portugal

3 Centro de Química Estrutural, Universidade de Lisboa, Instituto Superior Técnico, Av. Rovisco Pais, Lisbon 1049-001, Portugal

4 Department of Chemistry, University of Aveiro, Aveiro 3810-193, Portugal

5 LAQV-REQUIMTE, Department of Chemistry, NOVA School of Scienceand, Technology, NOVA University Lisbon, Caparica 2829-516, Portugal

Published online: 28 May 2025

Graphical Abstract

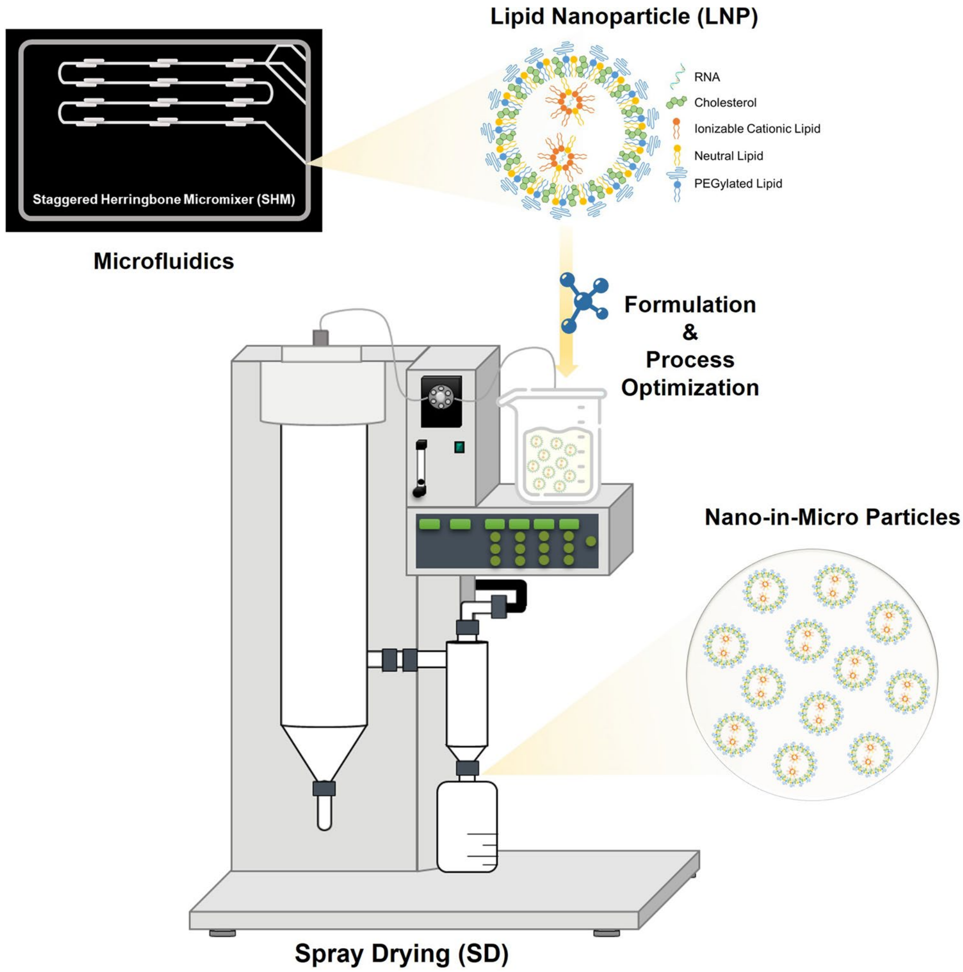

Keywords freeze drying · lipid nanoparticles · process and formulation development · RNA · spray drying

Introduction

Lipid nanoparticles (LNPs) are currently the preferred carrier for nucleic acid delivery [1, 2]. These delivery vehicles can protect the nucleic acid against degradation and facilitate their targeted delivery to specific cells or tissues [3]. However, marketed mRNA-LNPs still require conservative storage conditions (- 20 °C and—80 °C for Moderna and Pfizer/BioNTech COVID-19 vaccines, respectively), which are expensive and difficult to ensure [4]. Also, these requirements slow down and hamper the distribution of these therapeutics, especially in impoverished countries with insufficient storage facilities [5, 6].

Frozen storage is typically used to mitigate hydrolysis, which is the main source of mRNA instability [7]. Hence, water removal through drying may be considered as an alternative approach to enhance stability and extend shelf life [5–7]. Formulated as dry powders, mRNA-loaded LNPs could probably be distributed worldwide with a less conservative or absent cold chain supply. Nevertheless, biomolecules are exposed to different stress sources during drying process that may affect the dried product's critical quality attributes (CQAs) [8]. Process- and formulation-based strategies can be successfully leveraged to mitigate the effect of such stresses and enhance the storage stability of biopharmaceutical dry powders [8–10].

Various technologies are employed in the pharmaceutical industry to produce dry powders of biopharmaceuticals, with freeze drying (FD) being the gold standard approach [11]. In this process, the feed solution is typically loaded inside vials into the freeze dryer, frozen and subsequently dried by sublimation at low temperatures and under vacuum [12]. Despite the freezing stress involved, FD is considered a mild technology to process thermolabile biomolecules [8]. Additionally, the inherent high processing yields combined with established status within the pharmaceutical industry, including for aseptic processing, have positioned FD as the preferred technology to dry biomolecules [8]. Encouraging results have also been reported for nucleic acid-loaded lipid nanoparticles, with Pfizer announcing clinical trials for a freeze-dried Covid-19 vaccine formulation [13].

Spray drying (SD) is a particle engineering technology that presents several advantages over FD, including being a continuous process with higher throughputs, and the ability to tailor particle characteristics for diverse delivery routes (e.g., pulmonary) [14]. Despite being well-established in the pharmaceutical industry, SD is often disregarded for processing biomolecules due to the apparent high drying temperatures and atomization shear stresses [8]. Nevertheless, processing variables such as evaporative cooling, and short residence time enable SD as a mild technology [15, 16]. SD has been used to produce several commercial biopharmaceuticals, even under aseptic conditions [17]. More recently, at R&D environment, dried mRNA-LNPs for pulmonary delivery were produced by SD, using formulations comprising sugars and/or polyols (e.g., trehalose, mannitol) and amino acids (e.g., leucine and trileucine) [18, 19]. Moreover, Merkel and co-workers [20, 21] reported the use of SD to improve the stability of small interfering RNA (siRNA)-loaded LNPs for pulmonary delivery.

In the SD process, the feed solution is atomized in a nozzle placed at the top of a drying chamber to form fine droplets [22]. These droplets are subsequently dried with a drying gas stream, and the resulting dried particles are then separated from the gas stream, typically using a cyclone [22]. The atomization step is crucial, as it directly affects the particle characteristics of the dried product. The shear stress required to atomize the feed solution can also impact the stability of the biomolecules and nanoparticles [23]. Among atomizers, two fluid nozzles (2 FN) are the most commonly used. In these atomizers, droplets are formed due to the shear forces exerted by a high-velocity atomizing gas on the liquid surface [24, 25]. The resulting droplet size is directly proportional to the cap diameter and the feed flow rate (F_{feed}), while inversely proportional to the atomization gas flow rate (F_{atom}) [26].

The atomization ratio (R_{atom}) (Eq. 1), a metric of shear stress in 2 FN, indicates that higher R_{atom} values produce smaller droplets but also increase the product's exposure to greater shear stress [27]. Optimizing the R_{atom} in SD process is crucial to minimize the shear stress impact on the product. Additionally, formulation strategies incorporating amphiphilic excipients, such as surfactants, can be employed to further mitigate this effect [8, 28].

$$R_{atom} = \frac{F_{atom}}{F_{feed}} \tag{1}$$

This work focuses on the optimization of the SD process to enhance the stability and delivery potential of RNA-loaded LNPs. Microfluidics was primarily employed to produce neutrally charged, monodisperse populations of LNPs with Z-Average in the 40–200 nm range. The SD process and drying matrix were then fine-tuned to minimize the impact of shear stress during atomization, preserving LNPs'colloidal stability. Finally, SD was benchmarked against FD, as an alternative low-shear drying technology, to validate SD potential as a drying technology for RNA-loaded LNPs.

Materials and Methods

Materials

1,2-dioleoyl-sn-glycero-3-phosphoethanolamine (DOPE), 1,2-dioleoyl-3-trimethylammonium-propane (chloride salt) (DOTAP), and 1,2-Dimyristoyl-rac-glycero-3-methoxypolyethylene glycol-2000 (PEG-DMG 2000) were obtained from Avanti Polar Lipids. 1,2-distearoyl-sn-glycero-3-phosphocholine (DSPC) was purchased from Lipoid. EZ Cap™ EGFP mRNA (5-moUTP) was purchased from APExBIO. Ethanol 99% was bought from AGA. RiboGreen and TE-buffer were purchased from Thermo Fisher Scientific. Sucrose, poloxamer 188 (P188), cholesterol, sodium acetate anhydrous, tRNA, Triton X 100 and acetonitrile (ACN) were obtained from Sigma-Aldrich. Trehalose was obtained from VWR. Acetic acid glacial 100%, and leucine, were purchased from Merck. Poloxamer 407 (P407) was purchased from BASF. Triethylamine (TEA) was purchased from PanReac AppliChem. 10% SDS Solution was acquired from Bio-Rad.

Methods

Production of RNA-loaded Lipid Nanoparticles

Placebo and RNA-loaded LNPs were produced with a staggered-herringbone micromixer (SHM) microfluid chip from Dolomite (Dolomite, UK). The microfluidic chip was connected to 10 mL luer-lock disposable plastic syringes (HENKE-JECT®) (VWR, Portugal) containing the different aqueous and organic solutions, through a tube (inner diameter: 0.5 mm, outer diameter: 1.6 mm). The aqueous and organic flow rates were controlled by syringe pumps (NE-1000 SyringeONE Programmable Syringe Pump, New Era Pump Systems Inc., USA) at a 1556 μL min^{-1} and 444 μL min^{-1}, respectively. Aqueous phase consisted of 100 mM sodium acetate buffer pH 5.0 and the organic phase was prepared by mixing different mass ratios of lipids in ethanol. The organic solution was filtered through 0.45 μm filter (Millex-CV, Merck Millipore, USA) prior to each experiment to eliminate particles which might block the channels or influence flow conditions. The resulting aqueous dispersions of lipid nanoparticles were collected from the outlet tube and stored at 4 ºC, until further processing.

Stability tests

The storage stability of tRNA-loaded DOTAP-LNPs was evaluated for 16 weeks under different storage conditions: room temperature, 2—8 ºC, and −20 ºC without any stabilizing excipient. In this regard, the sample was divided into Eppendorfs and a different Eppendorf was taken from each condition and analyzed at each pre-determined timepoint. The stability of the LNPs was evaluated through DLS and EE analysis, according to the described methods in the following Sects. "Dynamic Light Scattering" and "Encapsulation Efficiency", respectively.

Spray Drying

A lab-scale Büchi spray dryer (Büchi, Switzerland) was used to produce different formulations of LNPs dry powders. The spray dryer was equipped with a two fluid nozzle (0.7/1.5 mm tip/cap) refrigerated by external water bath re-circulation. The spray drying unit was operated in open loop mode and the flow rate of drying nitrogen was set at 40 kg h^{-1}. Before initiating each experiment, the equipment was stabilized first with nitrogen gas and later with solvent until the outlet temperature (T_{out}) was constant. After stabilization, the feeding was commuted to the feed solution and the trial initiated. The mass feed flow rate to the nozzle was maintained with a peristaltic pump and the atomizing gas mass flow rate was varied throughout the experiments by adjusting the rotameter. Unless otherwise stated, all trials were performed with a R_{atom} of 4.6 and at an inlet temperature (T_{in}) of 120 ºC. The feed solution consisted of LNPs in different drying matrices. The dried product was separated from the gas stream in a high-performance cyclone and collected in plastic falcons. At the end of each trial, the feed solution was commuted to solvent to rinse the feed line and carry out a controlled shut down of the unit.

Shear Stress Test

The isolated effect of the spray drying atomization shear rate was evaluated through stress tests for different formulations. A two-fluid nozzle was used to atomize, at distinct R_{atom}, the feed solution into fine droplets, which were collected immediately after atomization. The impact of the atomization shear stress was evaluated on the atomized LNPs' hydrodynamic diameter (Z-Average) and polydispersity index (PdI) by DLS.

Freeze Drying

Lipid nanoparticles were lyophilized in a Virtis Advantage Freeze Dryer (SP Scientific Virtis, USA) coupled with a RV8 Vacuum pump from Edwards. Briefly, 1 mL of sample, consisting of LNPs in different drying matrices, was used for each trial, unless otherwise stated. Two different freezing cycles (A and B) were used to evaluate the impact of the freezing time. In cycle A (Fig. 1a), glass vials containing the samples were placed inside the freeze dryer, previously refrigerated to 4 ºC. After 1 h at 4 ºC, the freezing step started as the temperature decreased to −40 ºC over 1 h. After 5 h of freezing, primary drying proceeded at −40 ºC and 200 mTorr vacuum. After 36 h of primary drying, the temperature increased to 20 ºC over 2 h and secondary drying took place over 8 h. In cycle B (Fig. 1b), the glass vials containing the samples were frozen in a freezer at −80 ºC or −20 ºC overnight. After freezing, the vials were placed inside the freeze dryer, previously refrigerated to −40 ºC and the FD cycle was initiated. In this cycle, primary and secondary drying steps occurred under the same processing conditions described for cycle A.

Differential Scanning Calorimetry

The thermal stability of the different lipids was evaluated with differential scanning calorimetry (DSC) in a DSC 250 TA Instruments (TA Instruments, USA). Aluminum pinhole pans loaded with 3 to 5 mg of the sample material were used. The sample material was accurately weighed in a Mettler Toledo XPE26 analytical scale. The samples were equilibrated at −50 ºC, the temperature was modulated at 1 ºC every 60 s and then it was maintained constant for 1 min. Finally, the samples were heated at 2 ºC per minute until the temperature reached 250 ºC. The instrument was calibrated daily with indium.

Reconstitution of Lipid Nanoparticles Dry Powders

Before characterization, the dry powders were reconstituted with Milli-Q water at room temperature. The water was slowly injected through the wall of the vial and then the samples were slowly agitated by performing up & down movements with a micropipette. After complete reconstitution by visual inspection, the samples were analyzed.

Dynamic Light Scattering

Dynamic light scattering (DLS) was performed in a Zetasizer Nano ZS from Malvern (Malvern Instruments, UK).

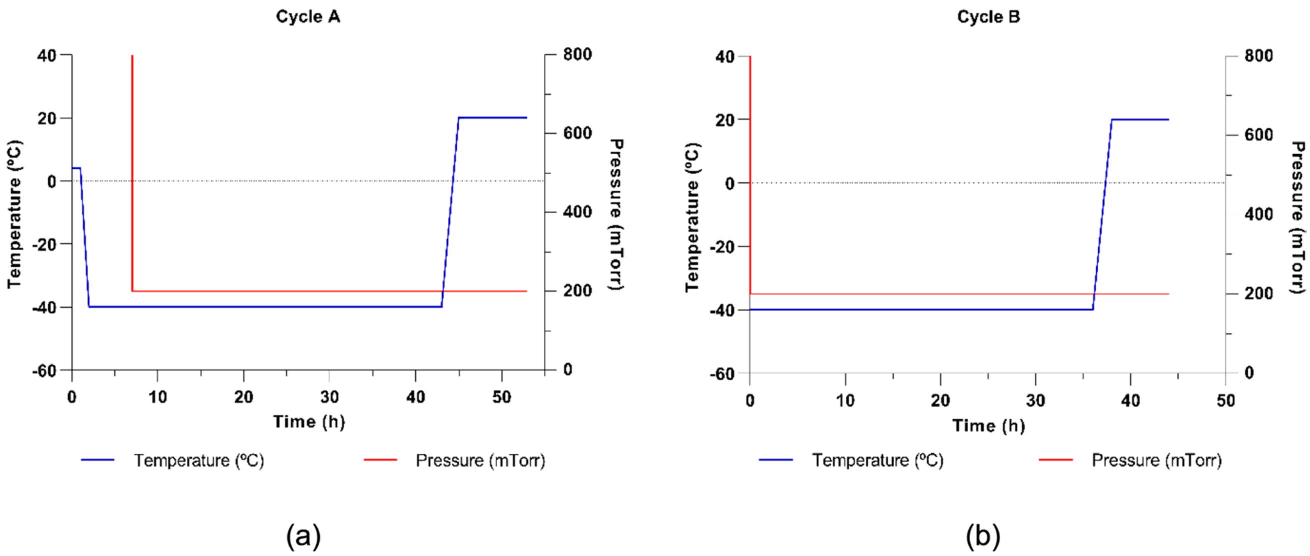

Fig. 1 Freeze drying cycles: **a** cycle A with the freezing step inside the FD and **b** cycle B with the freezing step at −80/−20 ºC, outside the FD

Z-Average and PdI were measured in disposable cells at a scatter angle of 173° assuming that the material was polystyrene latex (refractive index 1.590, absorption 0.010) and the dispersant was water (viscosity 0.8872 cP, refractive index 1.330). The measurements were made in triplicate at a temperature of 25 ºC with an equilibration time of 120 s. Zeta potential was measured in a folded capillary cell (DTS1070 from Malvern) assuming that the material was polystyrene latex, and the dispersant was water (dielectric constant 78.5). The measurements were made in triplicate at a temperature of 25 ºC with an equilibration time of 120 s.

Encapsulation Efficiency

The tRNA encapsulation efficiency (EE) was determined using the RiboGreen® assay (Quanti-IT™ RiboGreen®, Invitrogen, USA) in flat bottom black 96-well plates from ThermoFisher (ThermoFisher Scientific, USA). Samples were analyzed at a final tRNA concentration of 1 μg mL^{-1}. In half of the wells, 50 μL of 2% (v/v) of TE-Triton Buffer was added to lyse the lipid nanoparticles. 1% (v/v) TE-buffer was added to each well to achieve a final volume of 100 μL and the plate was then incubated at 37 ºC for 10 min. After incubation, 100 μL of 1% (v/v) RiboGreen reagent was added to each well and sample fluorescence measured at 25 ºC using a Synergy HTX microplate reader from BioTek (λem = 520 nm and λex = 480 nm) (Biotek, USA). Each sample was measured in triplicate and the tRNA concentration was determined using a standard curve. The tRNA encapsulation efficiency was calculated by the difference between the tRNA fluorescence in the presence and absence of TE-Triton Buffer (Eq. 2).

$$EE = \frac{Total\ tRNA - Unencapsulatedt\ RNA}{Total\ tRNA} \tag{2}$$

mRNA Integrity

mRNA integrity was assessed by reversed phase ion pair chromatography (RP-IP). The mRNA was extracted from the mRNA-LNP formulations using 0.1% SDS solution. Briefly, 0.1% SDS soliton was mixed with the mRNA-LNP sample (1:1 (v/v)) and vortexed for 15 s (VWR, Portugal). Sample separation was performed on a DNAPac RP column with 4-μm particles and dimensions of 2.1 × 100 mm (Thermo Fisher Scientific, USA) at a flow rate of 0.45 mL/minute and column temperature of 80 °C. Mobile phase A consisted of 0.1 M Triethylamine Acetate (TEAA) buffer and mobile phase B consisted of 50:50%v/v acetonitrile (ACN) (Sigma-Aldrich) and 0.1 M TEAA buffer. Separation was accomplished by step-gradient with an initial 2-min hold at 82.5% mobile phase A and 17.5% mobile phase B; a 5.0-min gradient from 17.5% to 45% mobile phase B hold for 3 min. Then, 0.1-min gradient to reach 100% ACN and hold for 4.9 min. At 15.10 min, a return to initial conditions of 82.5% mobile phase A and 17.5% mobile phase B in a 0.1-min gradient and hold for 1.9 min. Autosampler was kept at 4 °C to minimize mRNA degradation. Approximately, 0.01 μg of mRNA (10 μL of sample) were injected. mRNA was detected by UV at 260 nm. The chromatographs were collected, and the areas under the peaks were integrated using Empower Version 2.0 (Waters, Milford, MA, USA).

Results and Discussion

Spray Drying of Lipid Nanoparticles

tRNA-LNPs Production by Microfluidics and Stability

tRNA-loaded LNPs were prepared by microfluidics method using TFR = 2000 µL min^{-1} and FRR = 3.5:1 by adding the tRNA in the aqueous phase. tRNA-loaded DOPE and DOTAP-LNPs were produced with a N/P of 3. This N/P is being used in Onpattro® (siRNA-LNPs) which is closer in molecular weight to tRNA, when compared to mRNA (Table I) [29].

DOPE is an ionizable lipid, but it remains neutral at the working pH, making it unable to form complexes with tRNA and yielding a poor encapsulation efficiency within the LNPs. These findings are consistent with prior research, which highlighted the necessity of employing ionizable/cationic lipids that are positively charged at the working pH to encapsulate negatively charged nucleic acids within LNPs [30]. The increase in the Z-Average observed for DOPE-LNPs when tRNA was introduced in the processing aqueous stream may be related with process variability since no tRNA was encapsulated in the LNPs.

Oppositely, DOTAP demonstrated capability in encapsulating tRNA. Upon tRNA encapsulation, DOTAP-LNPs showed an increase in LNPs'Z-Average and PdI in comparison to the placebo nanoparticles produced under the same conditions, which is aligned with previous literature reports [31]. This increase in Z-Average for tRNA-loaded LNPs is likely a result of the tRNA being successfully encapsulated within the LNPs, as supported by the high tRNA encapsulation efficiency achieved (> 90%). Regarding the LNPs'surface charge, no significant differences were observed, as the LNPs maintained a neutral charge [32].

LNPs have been reported to be susceptible to both chemical and physical degradation [33]. Chemical degradation may include oxidation and hydrolysis while physical degradation typically includes aggregation, fusion, or leakage of encapsulated material [33]. For example, the siRNA-loaded LNPs formulation of Onpattro® presents a three-year shelf life when kept at 2–8 ºC and should not be frozen [34]. To optimize the storage conditions that would better maintain the LNPs' CQAs throughout the present study, the storage stability for tRNA-loaded DOTAP-LNPs was evaluated for different storage conditions (Fig. 2).

The tRNA-loaded LNPs stored at room temperature and at 2–8 ºC maintained consistent colloidal stability, as indicated by the unchanged Z-Average (from 48 to 62 nm) and PdI (from 0.160 to 0.205) values throughout the study period. This is in agreement with the report of Suzuki and coworkers [35], who did not observe any alteration in colloidal stability for similar LNPs stored at 4 ºC over an 18-month period.

For the samples stored at −20 ºC, an increase in both Z-Average (from 48 to 104 nm) and PdI (from 0.160 to 0.267) was observed immediately after the first timepoint, indicating the freezing/thawing of bare LNPs resulted a significant impact on colloidal stability. Up to the fourth week, the Z-Average remained practically unchanged, while after the fourth week an increasing tendency in both Z-Average and PdI was observed up to the final week. Nonetheless, the loss off colloidal stability upon frozen storage is expected as the formation of ice crystals and phase separation has been reported to negatively affect lipidic drug delivery systems [36–38]. However, some of the marketed RNA-LNPs therapeutics are being stored at −20 ºC/−80 ºC (e.g., Moderna and Pfizer/BioNTech Covid vaccines) while maintaining colloidal stability [39]. It is important to highlight that these marketed formulations also contain other excipients in their formulations, which may act as cryoprotectants and prevent loss of colloidal stability during storage at sub-zero temperatures [33, 39].

Regarding encapsulation efficiency, no differences were observed in the encapsulation efficiency during the time of the study as it remained above 98% for all storage conditions. Consequently, the increase in Z-Average and PdI observed for the LNPs stored at −20 ºC did not result in the leakage of the encapsulated nucleic acid. According to literature reports, the RNA release from LNPs during storage is not expected to occur [33].

Typically, biological molecules are maintained under cold storage conditions to prevent degradation [39, 40]. Considering that in this case, it was not possible to assess tRNA

Table I Z-Average, PdI, zeta potential, and encapsulation efficiency of DOTAP and DOPE-LNPs with tRNA loaded at an N/P of 3 and placebo

Ionizable/cationic lipid	Z-Average (nm)		PdI		Zeta Potential (mV)		Encapsulation Efficiency (%)	
	N/P = 3	Placebo	N/P = 3	Placebo	N/P = 3	Placebo	N/P = 3	Placebo
DOTAP	46.8 ± 0.4	38.0 ± 0.1	0.13 ± 0.01	0.10 ± 0.00	1.1 ± 0.1	−0.6 ± 0.8	98.9 ± 0.4	NAP
DOPE	84.7 ± 0.5	78.4 ± 0.8	0.21 ± 0.01	0.17 ± 0.01	−0.1 ± 0.0	−0.2 ± 0.1	NAP	NAP

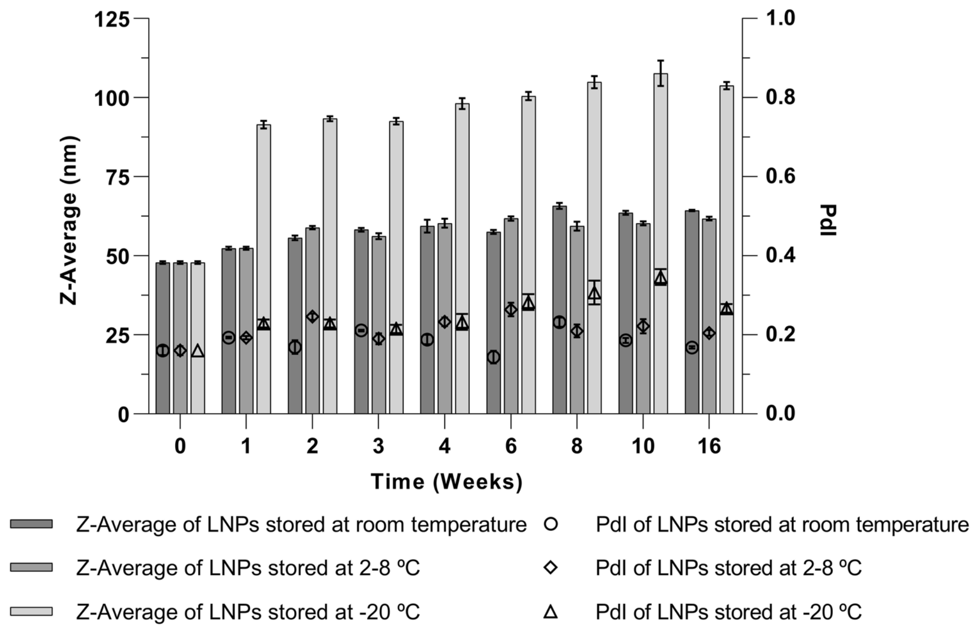

Fig. 2 tRNA-loaded DOTAP-LNP's Z-Average and PdI stored at room temperature (20–25 ºC), 2–8 ºC, and −20ºC without stabilizing excipients. Data presented corresponds to the mean and standard deviation

integrity for the different storage conditions and that no significant differences were observed in terms of colloidal stability between room temperature and 2–8 ºC, the latter is suggested as storage condition for following studies as a conservative approach. However, the combination of formulation and processing rendered LNPs' able to maintain the encapsulation efficiency of the nucleic acid even at room temperature.

Process Optimization

Different experiments were carried out to optimize the SD process for LNPs, while considering the impact of shear stress and thermal stress on their colloidal stability (Table II). All experiments were carried out using a standard drying matrix formulation of 10% (w/v) of trehalose, as it has been previously used to dry different lipid-based systems [36–38, 41, 42].

The first set of experiments focused on evaluating the impact of shear stress by adjusting the atomizing gas flow rate while maintaining a constant feed rate (Table II). The decrease in R_{atom} resulted in the formation of larger droplets, requiring higher temperatures during drying. To address this, a compromise was made by increasing the temperature to avoid wetting the SD chamber walls.

While trials A and B were successfully performed, trials C, D, and E encountered processing limitations. The incomplete drying of the produced droplets was primarily observed visually, as droplets were noted along the walls of the drying chamber – an indicator of suboptimal drying conditions during the spray drying process. Visual observations strongly suggested incomplete evaporation, likely due to process parameters such as lower atomization ratio (larger droplets), insufficient inlet temperature, inadequate residence time, or chamber length.

During the SD process, temperature can potentially cause lipid phase transitions in the LNPs, leading to fusion, aggregation, or alterations in the LNPs' structure [43]. These changes could impact the colloidal stability and the integrity of the encapsulated biomolecule [43]. However, no correlation was found between the inlet temperature and the Z-Average nor PdI. These findings are likely correlated with factors such evaporative cooling and short residence times, which reduced the LNP's thermal exposure during the SD process [44, 45].

Table II DOPE-LNPs' Z-Average and PdI before and after spray drying trials A-E

Trial	T_{in} (°C)	R_{atom}	Z-Average before SD (nm)	PdI before SD	Z-Average after SD (nm)	PdI after SD
A	70	8.3	66.2 ± 0.44	0.22 ± 0.01	187.9 ± 17.2	0.57 ± 0.10
B	120	4.6	62.0 ± 1.01	0.21 ± 0.00	177.3 ± 7.35	0.59 ± 0.05
C	140	2.8	62.0 ± 1.01	0.21 ± 0.00	150.8 ± 3.8	0.25 ± 0.01
D	150	2.8	62.1 ± 0.55	0.18 ± 0.00	176.0 ± 1.9	0.33 ± 0.01
E	180	2.8	66.4 ± 0.91	0.22 ± 0.01	156.3 ± 1.5	0.30 ± 0.01

Regarding shear stress, trial B, performed at a lower R_{atom}, appeared to be more suitable for drying the LNPs compared to Trial A, as it resulted in a smaller increase in Z-Average. Based on the data, LNPs seemed to be more susceptible to the atomization shear stress than temperature stress. To further validate this hypothesis, the effect of shear stress on LNPs'colloidal stability was evaluated by atomizing the feed solution at different R_{atom} and collecting the atomized solution without drying for DOPE and DOTAP-LNPs in a 10% (w/v) trehalose formulation (Fig. 3).

A noticeable impact of shear stress was observed on the colloidal stability of LNPs at R_{atom} higher than 4.6, suggesting that this LNPs' formulation is sensitive to shear stress. This susceptibility may be attributed to their aqueous core, which imparts a more fluid nature compared to solid LNPs [46, 47]. Although it is critical to decrease the R_{atom} to mitigate the effect of shear stress, such reduction will originate larger droplets that may impact drying efficiency and introducing limitations to the process. Therefore, a balance between R_{atom} and temperature is required to minimize shear stress, while ensuring that the droplets dry effectively. These findings align with the aforementioned data and reinforce the decision to select the processing conditions of trial B for subsequent trials.

Drying Matrix Optimization

Since it was previously observed that the LNPs are particularly susceptible to shear stress, the effect of leucine and different surfactants was evaluated in combination with trehalose (Fig. 4). It is important to notice that for leucine, trehalose's concentration was adjusted due to solution's solubility limits.

The combination of 1% (w/v) leucine with trehalose resulted in a destabilizing behavior that led to the complete loss of LNPs' colloidal stability after drying. Employing trehalose as drying matrix without additional excipients, resulted in a particle size of approximately 177.3 ± 7.4 nm. This value is substantially lower than the pronounced increase to 999.0 ± 187.5 nm observed when leucine was added. Leucine is hydrophobic and may interfere with the lipid matrix leading to coalescence of LNPs. This outcome suggests that the particle size increase is primarily due to leucine and not a result of reduced trehalose concentration. It is worth emphasizing that the reduction of the sugar concentration was related to leucine water solubility constraints. Nonetheless, leucine has been used as SD matrix for SLNs and has been reported to significantly mitigate the Z-Average's increase for formulations with more than 20% (w/w) of leucine [48]. Possibly, in this case, leucine crystals were additionally formed during the SD process and induced alterations in the lipid matrix that led to the loss of colloidal stability [14, 49].

Pertaining to P407, it did not improve noticeably the colloidal stability of LNPs, when compared to trehalose-only control, resulting in polydisperse populations. The combination of 0.1% (w/v) P188 with 10% (w/v) trehalose stood out as the only matrix capable of maintaining the monodispersity of LNPs after SD.

Regarding P188, the shear-protective effect may not be the only stabilization mechanism responsible for the maintenance of colloidal stability [50–52]. Studies performed by Maskarinec and coworkers [51], revealed that P188 selectively inserts into bilayer membranes where the local lipid packing density is reduced, helps to increase the local packing

Fig. 3 Z-Average and PdI of DOPE and DOTAP-LNPs subjected to different R_{atom} in a 10% (w/v) trehalose formulation. Data presented corresponds to the mean and standard deviation

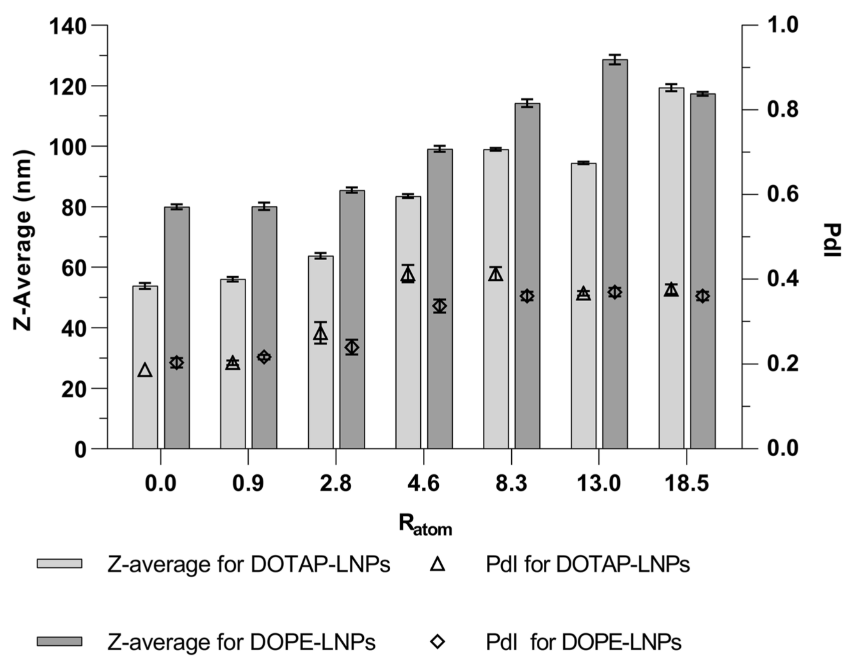

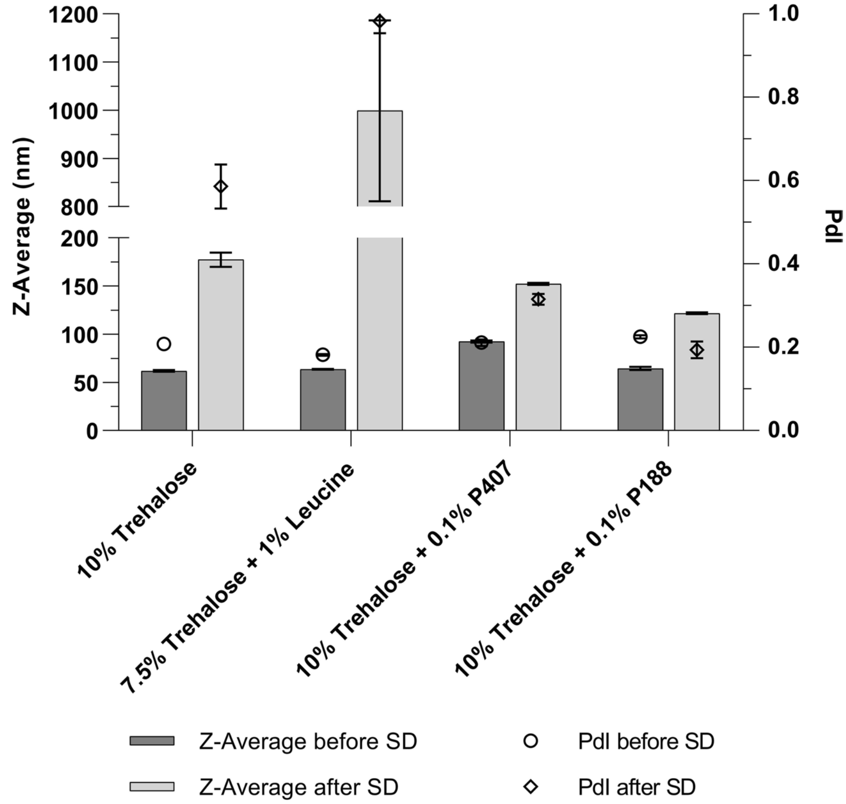

Fig. 4 Effect of different shear protecting excipients on LNPs colloidal stability of DOPE-LNPs after spray drying. Data presented corresponds to the mean and standard deviation

density and is squeezed out once the membrane is healed. Adhikari *et al.* [52] later confirmed this mechanism with computer simulations and observed that the P188 hydrophobic chains insert themselves into damaged lipid layers and close any opened pores. Additionally, Trenkenschuh and coworkers [53] observed a significant increase in colloidal stability of extracellular vesicles during FD when 0.02% (w/v) P188 was used in combination with 5% (w/v) sucrose, which was also justified with P188 insertion within the lipid layers.

Although the difference while employing P407 or P188 may appear small in Fig. 4, there are variations in Z-average (152.3 ± 1.2 nm for P407 and 121.8 ± 0.8 nm for P188) and more evident variances in the polydispersity index. For P407, the PdI exceeded 0.3, indicating a heterogeneous size distribution with multiple populations observed during dynamic light scattering measurements. In contrast, P188 exhibited a PdI of approximately 0.20, which suggests a more monodisperse population with a narrower size distribution. These differences are worth emphasizing as they could influence the formulation's overall stability and performance. While the difference in Z-average may not seem significant, the distinct variation in size distribution (indicated by PdI) and the presence of multiple populations with P407 underline the different physicochemical characteristics of the two excipients.

The surfactants concentration is known to play a critical role in maintaining or disrupting the colloidal stability of lipid systems. Surfactant's micelles – formed at concentration above the critical micelle concentration (CMC) – have been reported to induce stress in lipid membranes that may cause its disruption, as demonstrated by Triton X-100 being used extremely above its CMC to lyse lipid systems and release the encapsulated nucleic acid [54–57]. Therefore, the higher CMC of P188 compared to P407 (i.e., 0.125 mM and 0.05 mM for P188 and P407, respectively) may justify the differences in the stabilizing behavior as the 1% (w/v) used is slightly above the CMC for P407 and borderline the CMC of P188 [51, 58].

Since the surfactant concentration plays such important role in the LNPs' stabilization and should be assessed case by case, a further optimization was performed where both trehalose and P188 concentrations were varied (Table III, Fig. 5).

Within the tested range, the drying matrix that resulted in the better maintenance of LNPs' colloidal stability was the combination of 10% (w/v) trehalose with 0.1% (w/v) P188. This drying matrix not only led to the smallest increase in Z-Average after SD, but also resulted in a monodisperse population with no increase in the PdI. Despite the 30% (w/v) trehalose with 0.05% (w/v) P188 drying matrix showing similar results concerning colloidal stability, the 10% (w/v) trehalose with 0.1% (w/v) P188 allowed a better compromise between maintenance of colloidal stability and acceptable solution viscosity. Additionally, P188's optimal concentration to stabilize

Table III Effect of trehalose and P188 concentration on Z-Average and PdI of DOPE-LNPs after spray drying

Trehalose %(w/v)	P188 %(w/v)	Z-Average (nm)	PdI
10	0.1	121.8 ± 0.8	0.19 ± 0.02
10	0.25	143.8 ± 1.0	0.17 ± 0.03
10	0.5	154.7 ± 1.4	0.22 ± 0.02
20	0.5	133.0 ± 2.5	0.21 ± 0.02
30	0.1	143.2 ± 1.8	0.32 ± 0.01
30	0.05	122.7 ± 1.1	0.21 ± 0.01

these LNPs appears to be very proximal to the surfactants' CMC. This can be an indicator that it is the highest concentration that can be used without forming micelles, which have been reported to destabilize lipid layers [51].

The initial shear stress test was repeated with the optimized formulation to validate the shear-protective behavior of P188 (Fig. 5).

As expected, the incorporation of 0.1% (w/v) P188 in the drying matrix decreased the impact of the shear stress during atomization and substantially improved the LNPs colloidal stability of both DOPE and DOTAP-LNPs. For both sugar formulations without P188, a noticeable impact on LNPs colloidal stability was evident at R_{atom} higher than 4.6. However, when P188 was incorporated in the drying matrix the increase in Z-Average was minimized and PdI remained below 0.3, even at an R_{atom} of 18.5. These findings strongly demonstrate the stabilization potential of P188 for LNPs.

Considering that sucrose has been extensively used to stabilize lipid systems compared with trehalose (including in marketed formulations), one additional trial was performed to benchmark both sugars in combination with 0.1% (w/v) of P188 (Fig. 6) [7, 41, 53, 59].

The use of sucrose in the formulation resulted in a lower increase in the LNPs' Z-Average after SD compared to trehalose. While the differences in PdI are small, the Z-average data after spray drying reveal substantial distinctions. Specifically, trehalose in combination with P188, resulted in a Z-average of 179.8 ± 2.7 nm and PdI 0.20 ± 0.02, while sucrose with P188 yielded LNPs with a Z-average 125.5 ± 2.4 nm and PdI 0.22 ± 0.02, after spray drying. The differences in the stabilizing behavior of both sugars may be justified with sucrose's enhanced ability to form hydrogen bonds with the phospholipids' headgroups, which results in extensive molecular interactions and reduces the nanoparticle mobility [60].

To understand the impact of PEGylation on LNPs' colloidal stability before and after SD, the PEGylated lipid molar ratio was varied for tRNA-loaded DOTAP-LNPs, maintaining sucrose in combination with 0.1% (w/v) P188 as drying matrix (Fig. 7). Polyethylene glycol (PEG) is the most common "stealth" polymer in the drug delivery field, due to its established safety profile in humans and its classification as Generally Regarded as Safe (GRAS) by the FDA [61]. In lipid nanoparticles formulations, PEG lipids are essential components as they control LNPs size and provide stabilization by acting as a steric barrier, preventing aggregation during storage [29, 61–63]. Additionally, PEG-lipids

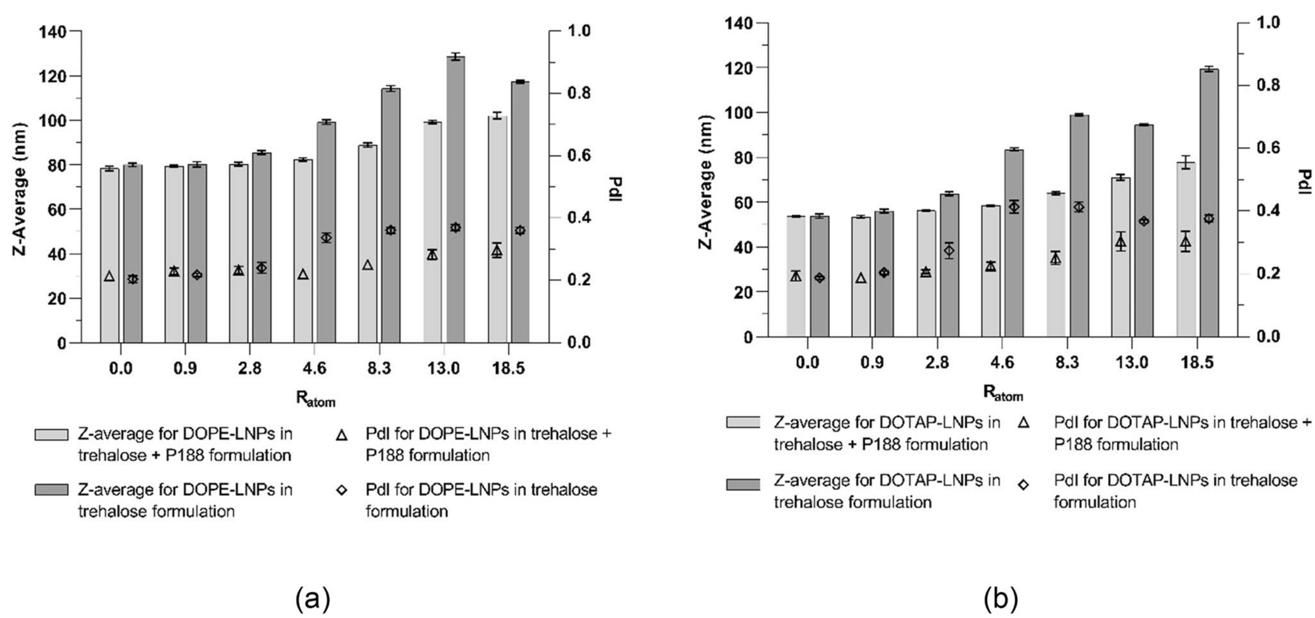

Fig. 5 Shear protective effect in the Z-Average and PdI of P188 for **a** DOPE and **b** DOTAP-LNPs. Data presented corresponds to the mean and standard deviation

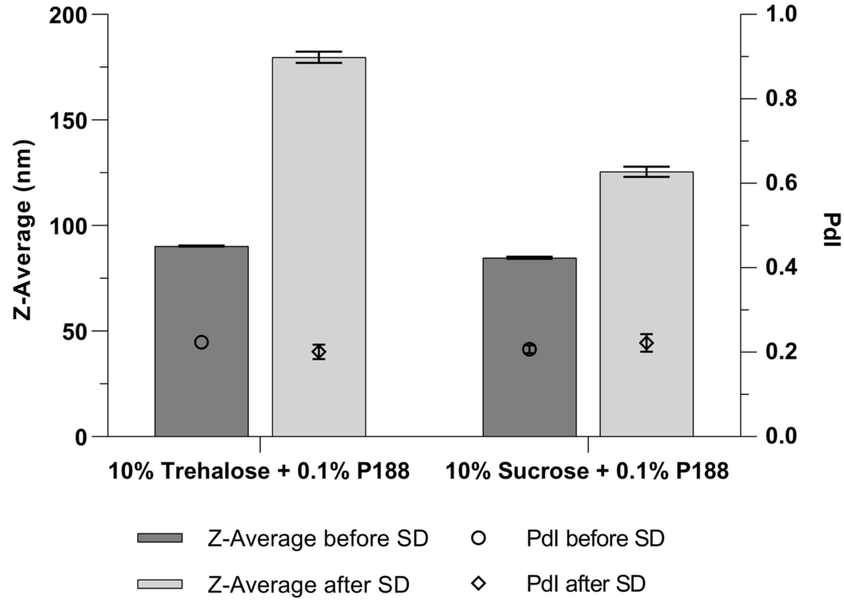

Fig. 6 Z-Average and PDI of DOPE-LNPs before and after SD using 10% (w/v) of trehalose or sucrose in combination with 0.1% (w/v) P188 as drying matrices. Data presented corresponds to the mean and standard deviation

enhance circulation time by reducing opsonization, limiting clearance by reticuloendothelial cells, and mitigating rapid uptake, thereby improving the LNPs' circulation half-life [61, 63, 64]. However, this also hinders endosomal release by obstructing membrane fusion between the LNPs and the endosomal membrane. Therefore, the type and amount of PEG lipids must be carefully adjusted to balance sufficient stealth and stabilization effects without hindering cargo release, a phenomenon known as the "PEG Dilemma" [64].

No trends in Z-Average or PdI of DOTAP-LNPs were identified with varying PEGylated lipid molar ratios after microfluidics. DOTAP-LNPs consistently presented low values across all tested ranges, suggesting that the surface area-to-volume ratio was already small enough to prevent repulsions between PEGylated lipid side chains, thus not affecting the Z-Average. However, a significant increase in PdI was observed after SD, with some conditions resulting in polydisperse populations.

Regarding zeta potential, a decreasing tendency towards 0 mV was identified with increasing PEGylated lipid molar ratios, yet the LNPs remained neutral throughout the tested range. Additionally, the SD process did not affect the zeta potential, and all formulations remained neutral, consistent with literature reports.

For DOTAP-LNPs, high tRNA encapsulation efficiency (> 99%) was achieved for PEGylated lipid molar ratios up to 5%, with a slight decrease to 97% at 10%. No considerable variation in encapsulation efficiency was observed after SD, aligning with previous observations for Z-Average. Moreover, it is worth mentioning that in these trials, the incorporation of the surfactant P188 (0.1% (w/v)) consistently demonstrated that it did not destabilize the LNPs nor promoted RNA leakage under the tested concentration range.

While these results provide valuable insights into the physicochemical properties of DOTAP-LNPs as a function of PEGylated lipid content, further *in vitro* studies would be necessary to evaluate the biological impact of PEGylation. Adverse effects such as anti-PEG antibody production, impaired cellular internalization, and decreased intracellular protein expression of mRNA have been reported at high molar ratios [65–67]. Since no enhanced stabilization effect was observed during the SD process for different PEGylated lipid molar ratios, a 1.5% ratio was considered for the following studies, as it is already approved in commercial formulations [33].

Benchmarking Spray Drying With Freeze Drying

Currently, FD is still considered the gold standard drying technology for biopharmaceuticals, one of the main reasons being the absence of process-induced shear stress that can compromise the integrity of large molecules [8]. However, spray drying is an attractive alternative, particularly for large-scale production, due to its higher throughput, cost-effectiveness, and better control of powder properties (e.g., particle size, density) [8]. Therefore, to compare the results obtained with SD with the gold standard FD, various formulations previously used were tested with FD on DOPE and DOTAP-LNPs'colloidal stability (Fig. 8). A standard FD cycle, representative of an industrial process, was employed (cycle A).

Freeze drying LNPs without stabilizing excipients led to a major increase in Z-Average and PdI, causing the loss of colloidal stability. This finding aligns with Suzuki *et al.*' [68] observations, where similar nanoparticles without stabilizing excipients showed increased Z-Average and PdI after

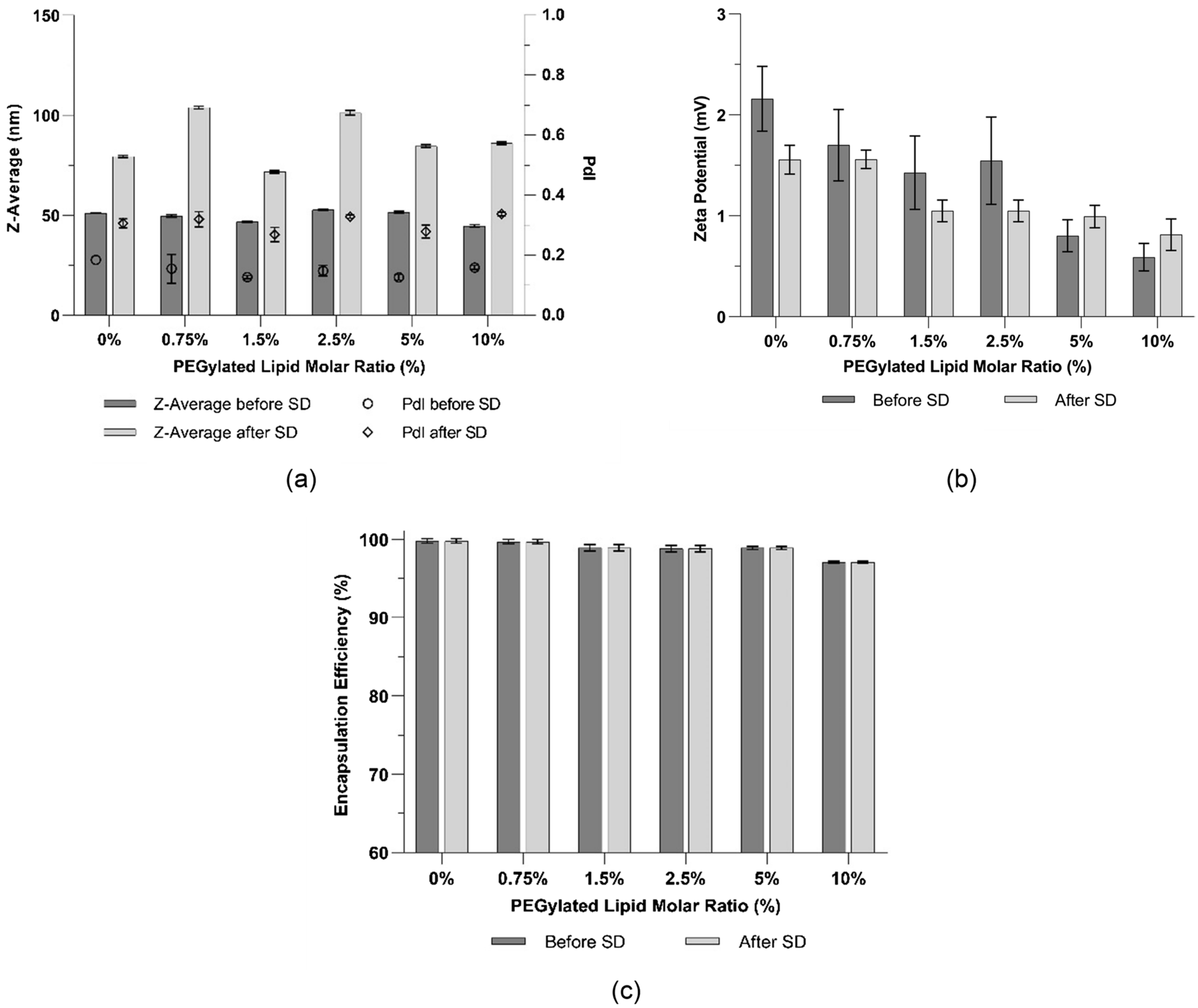

Fig. 7 **a** Z-Average and PdI, **b** zeta potential and **c** encapsulation efficiency of DOTAP-LNPs with different pegylated lipid molar ratios, before and after SD

FD. This increase in Z-Average associated with the loss of colloidal stability is likely due to fusion or aggregation and may ultimately lead to the leakage of the encapsulated material [36, 69]. However, when sugars were used as drying matrices, the increase in Z-Average and PdI was minimized, indicating better stability compared to bare LNPs, which is consistent with Suzuki *et al.*'s findings [68].

While trehalose and sucrose are commonly used stabilizing excipients in FD, sucrose exhibited a more pronounced stabilizing effect than trehalose, maintaining colloidal stability after FD [6, 37]. Both sugars are reported to form glass matrices that immobilize nanoparticles, preventing fusion/aggregation, and protecting against mechanical stresses caused by ice crystal formation [37]. Although, to the best of our knowledge, no literature reports the superior stabilizing potential of sucrose compared to trehalose during FD of LNPs, several authors report similar findings for different lipid systems (e.g., liposomes and SLNs) [70, 71]. Molecular dynamic simulations suggest that sucrose's stronger interactions with the LNPs'surface, forming 10% more hydrogen bonds with phospholipids headgroups compared to trehalose, may justify the different stabilizing behaviors [60].

The incorporation of P188 in the FD matrix yielded contradictory results for DOPE-LNPs and DOTAP-LNPs. While for DOTAP-LNPs, P188 did not produced any significant effect, when combined with 10% (w/v) trehalose it mitigated the increase in LNPs' z-average after FD. On the other hand, the effect of P188 in sucrose formulations was minimal, and differences may be attributed to process variability rather than stabilization effects.

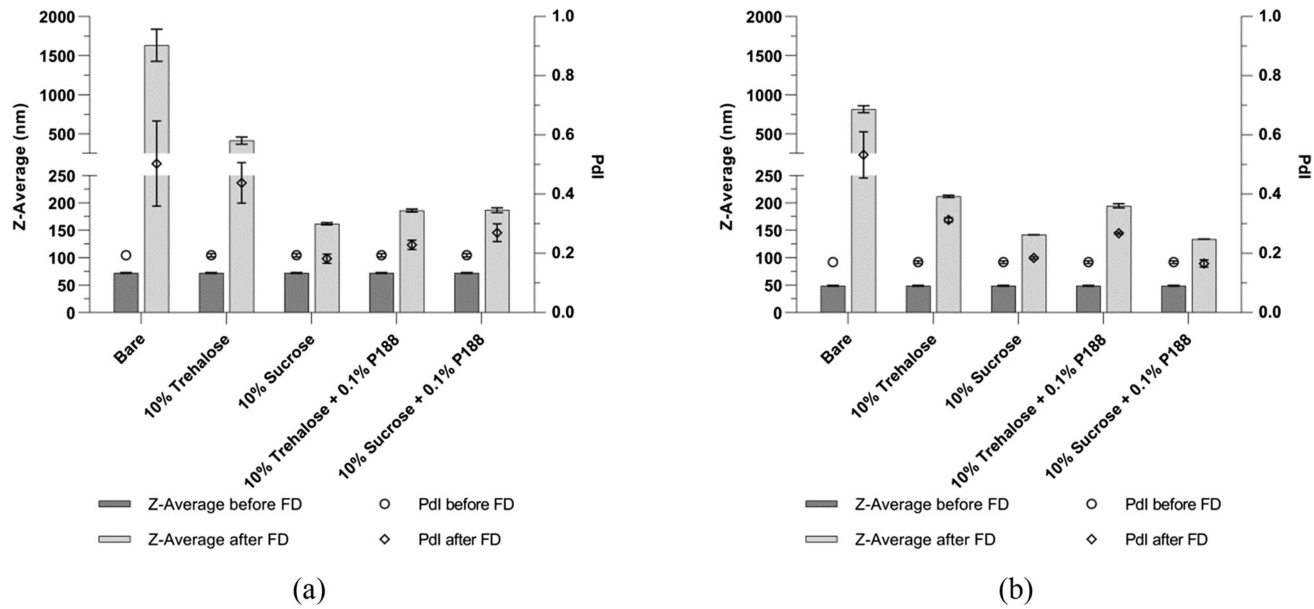

Fig. 8 Z-Average and PdI of **a** DOPE and **b** DOTAP-LNPs freeze dried in different drying matrices, using FD cycle A

Table IV Melting transitions of the different lipids obtained by differential scanning calorimetry

Lipid	DSPC	Cholesterol	PEG-DMG2000	DOPE	DOTAP
$T_{melting}$ (°C)	108.5	147.0	48.6	−25.6	8.0

In the FD process, temperature changes can potentially lead to lipid phase transitions, which, in turn, may cause alterations in the LNP structure. Both DOTAP and DOPE (Table IV) exhibited melting transitions between room temperature and primary drying temperature during FD, which is consistent with what previous literature reports have found [72]. Since both lipids are the main components of the LNPs, their respective phase transitions are likely to impact the LNPs' colloidal stability. However, it is important to note that DOTAP's melting transition occurred at 8 ºC, whereas DOPE's occurred at −25.6 ºC. Therefore, it is more likely that the presence of sucrose and trehalose, which were used as cryoprotectants in the drying matrix, might have prevented phase transitions in DOTAP-LNPs more effectively compared to DOPE-LNPs [73]. This could help explain the higher increase in Z-Average observed after FD for DOPE-LNPs.

tRNA EE was measured before and after FD to evaluate if the process resulted in leakages of the encapsulated material. For DOTAP-LNPs, the tRNA encapsulation efficiency remained practically unchanged after freeze drying (> 97%), indicating that even for the formulations were colloidal stability was lost, no encapsulated material was released (Table V). Additionally, the LNPs' zeta potential was also not affected by FD as the LNPs remained neutral after processing.

The impact of the freezing rate was also evaluated on DOPE-LNPs. Sucrose and trehalose were used as drying matrices for three different freezing protocols i.e., (a) freezing in a precooled freezer to −80 ºC (cycle B), (b) freezing in a precooled freezer to −20 ºC (cycle B) and (c) freezing down to −40 ºC at approximately 0.7 ºC min^{-1} (cycle A) (Fig. 9).

An increase in Z-Average was observed with the decrease in the freezing rate, demonstrating the impact of the freezing rate on LNPs' colloidal stability after FD. These results are aligned with literature, which suggests that slow freezing rates can lead to the formation of large ice crystals and non-uniform distribution of cryoprotectants, potentially disrupting lipid membranes and causing a loss of colloidal stability for LNPs [36, 38, 69]. Notably, the trehalose formulation presented a much more pronounced increase in Z-Average and PdI, indicating its inability to maintain LNPs'colloidal stability under any freezing protocol. In contrast, the sucrose formulation consistently yielded monodisperse populations with Z-Average values below 200 nm, regardless of the freezing protocol used. This difference in behavior could be attributed to trehalose's tendency to crystallize upon freezing, which may have compromised its stabilizing potential [74].

Remarkably, regardless of the freezing rate, the Z-Average of LNPs in the sucrose formulation remained consistent. This suggests that the sucrose formulation

Table V Zeta Potential of DOPE and DOTAP-LNPs and encapsulation efficiency of DOTAP-LNPs freeze dried in different drying matrices with standard FD cycle A

			Encapsulation Efficiency (%)	Zeta potential (mV)
DOPE	**Before FD**		NAP	−0.1 ± 0.01
	After FD	Bare		−0.6 ± 0.03
		10% (w/v) trehalose		−0.1 ± 0.01
		10% (w/v) sucrose		−0.2 ± 0.03
		10% (w/v) trehalose + 0.1% (w/v) P188		−0.1 ± 0.03
		10% (w/v) sucrose + 0.1% (w/v) P188		−0.2 ± 0.04
DOTAP	**Before FD**		98.1 ± 0.3	1.9 ± 0.55
	After FD	Bare	98.3 ± 0.3	1.1 ± 0.13
		10% (w/v) trehalose	97.5 ± 0.6	1.2 ± 0.07
		10% (w/v) sucrose	97.1 ± 0.8	1.0 ± 0.04
		10% (w/v) trehalose + 0.1% (w/v) P188	98.2 ± 0.6	1.1 ± 0.05
		10% (w/v) sucrose + 0.1% (w/v) P188	97.4 ± 1.0	0.9 ± 0.12

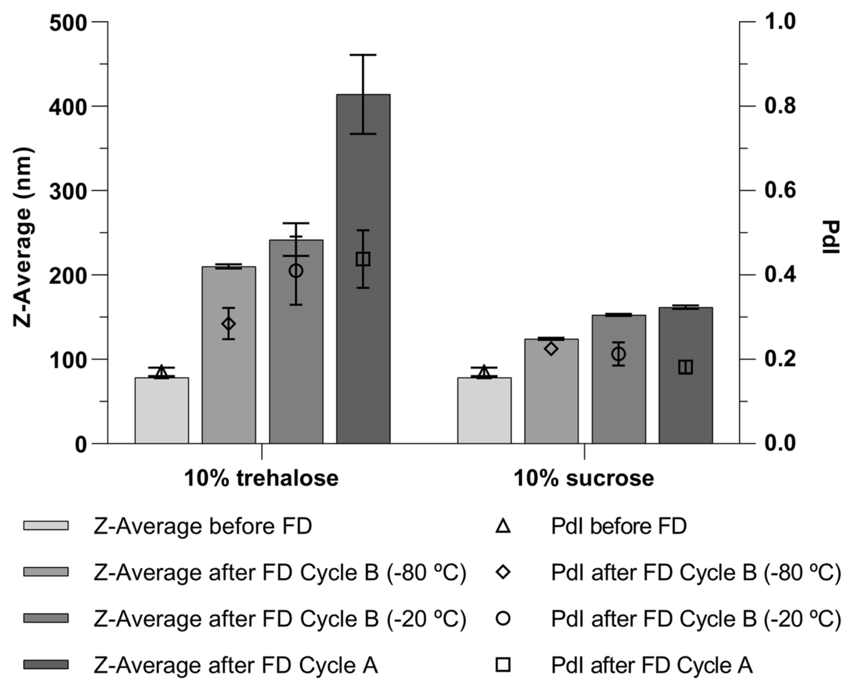

Fig. 9 Effect of the freezing temperature on DOPE-LNPs' Z-Average and PdI. Data presented corresponds to the mean and standard deviation

successfully mitigated the potential stresses associated with slow freezing rates. Consequently, the drying stress might be the only factor influencing the LNPs'colloidal stability in this case. It is worth noting that both Moderna and Pfizer/BioNTech Covid vaccines employ a sucrose-containing formulation for frozen storage [7]. Thus, any increase in particle size during the thawing process is not expected. Additionally, an increase in size after lyophilization of similar LNPs has been documented in the existing literature without compromising mRNA expression [13].

With the impact of formulation and process variables assessed for FD, the results from the two technologies explored in this work were benchmarked. By comparing SD and FD results from DOPE-LNPs in 10% (w/v) trehalose, it was noticeable that although both technologies yielded polydisperse populations, SD resulted in LNPs with a lower z-average after reconstitution (177.3 ± 7.4 nm *vs.* 414.2 ± 46.9 nm). However, when adding P188 to the drying matrix formulations, the differences between both technologies are eliminated and LNPs colloidal stability was maintained (186.3 ± 2.7 nm and 0.27 ± 0.03, for z-average and PdI after FD; and 179.8 ± 2.7 nm and 0.20 ± 0.02 for z-average and PdI after SD). During the SD trials, it was thought that P188's stabilizing effect was related with its ability to protect LNPs' against the atomization shear stress. Nevertheless, the incorporation of P188 in the FD formulations suggests that it can serve as a stabilizer against various types of stress beyond shear stress.

Regarding drying matrix formulations consisting of the combination of either trehalose or sucrose with P188, for SD the differences between both sugars were notorious, with sucrose rending particles with smaller Z-Average after reconstitution (125.5 ± 2.4 nm vs. 179.8 ± 2.7 nm). On the other hand, FD with either trehalose or sucrose in combination with P188 produced comparable results (186.3 ± 2.7 nm for trehalose vs. 187.0 ± 4.4 nm for sucrose).

Finally, by comparing both technologies using similar formulations (Table VI), it can be concluded that SD is able to assure identical colloidal stability of LNPs after reconstitution compared to FD. Moreover, SD yielded LNPs with smaller Z-average when compared to FD while employing the freezing protocol corresponding to cycle A. In cycle A, the freezing step occurred inside the freeze drier at a freezing rate of approximately 0.7 ºC min-1 until it reached—40 ºC. This corresponds to a slow freezing rate which could induce phase separation, leading to higher particle size increase. On the other hand, the swift evaporation in spray drying may circumvent those issues and mitigate the increase in Z-average. These are key results as SD is usually perceived as a more harmful drying technology than FD due to the shear stress imposed to the feed solution to promote the required atomization. Results from the present work indeed show an effect of atomization shear stress on the final properties of tRNA-loaded LNPs, but also that through formulation and process optimization it is possible reduce its impact to levels comparable to the FD gold standard. Therefore, the present work supports that SD can be an enabling technology for drying RNA-loaded lipid nanoparticles, presenting clear advantages over FD, as it is able to yield material with similar CQAs than the former but with a better industrialization potential. Future research should focus on formulation and process optimization to further minimize the impact of the spray drying process on product quality across different RNA types (e.g., mRNA) and evaluate the impact of process scale-up in the final properties of LNP-based formulations.

Drying of mRNA-Loaded Lipid Nanoparticles

Microfluidics was employed to produce mRNA-loaded lipid nanoparticles at a target mRNA concentration of 0.1 mg mL^{-1}, comparable to the marketed approved mRNA-LNPs [29]. Then, the mRNA-LNPs were subsequently dried through the two drying techniques: spray drying and freeze drying, using the optimized process conditions and employing a 10% (w/v) sucrose and 0.1% % (w/v) P188 drying matrix. Each resulting powder was reconstituted and characterized (Table VII).

Similar to what has been observed for tRNA-loaded lipid nanoparticles, both SD and FD increased the mRNA-loaded LNPs' Z-Average. This increase in Z-average particle size post drying is consistent with findings reported in the literature [18, 20]. Nonetheless, LNPs' colloidal stability was maintained in both SD and FD technologies, since monodisperse populations were obtained (PdI < 0.3).

mRNA encapsulation efficiency was also affected by the drying process and unlike what was reported for tRNA, a decrease was observed after both SD and FD, being more pronounced in the latter. Although process conditions could be further optimized to minimize the impact, the decrease in

Table VI Z-Average and PdI of DOPE-LNPs after spray drying and freeze drying

Technology	Drying cycle	Drying matrix	Z-Average (nm)	PdI
SD	NAP	10% (w/v) sucrose + 0.1% (w/v) P188	125.4 ± 2.4	0.22 ± 0.02
FD	A	10% (w/v) sucrose	162.0 ± 2.1	0.18 ± 0.02
		10% (w/v) sucrose + 0.1% (w/v) P188	187.0 ± 4.4	0.27 ± 0.03
	B (−20 ºC)	10% (w/v) sucrose	152.6 ± 1.4	0.21 ± 0.03
		10% (w/v) sucrose + 0.1% (w/v) P188	129.1 ± 1.5	0.16 ± 0.00
	B (−80 ºC)	10% (w/v) sucrose	124.4 ± 1.4	0.23 ± 0.01

Table VII Z-Average, PdI, mRNA encapsulation efficiency and mRNA integrity for mRNA-loaded LNPs after microfluidics, spray drying and freeze drying (cycle A) in a 10%(w/v) sucrose and 0.1% % (w/v) P188 drying matrix

Processing stage	Z-Average (nm)	PdI	mRNA EE (%)	mRNA integrity (%)
Microfluidics	80.0 ± 2.7	0.19 ± 0.02	95.6 ± 0.1	82.1 ± 0.2
Spray drying	124.3 ± 2.9	0.21 ± 0.04	86.1 ± 0.2	82.6 ± 0.6
Freeze drying	101.0 ± 0.5	0.21 ± 0.01	68.0 ± 1.2	85.7 ± 0.3

EE after drying is expected and has been previously reported in literature [75–77].

Regarding the mRNA integrity, the microfluidics and SD and FD processes did not result in substantial mRNA degradation as both present results similar to the unprocessed standard. These are very promising results because, despite the small decrease in encapsulation efficiency, mRNA integrity was still maintained after SD and FD. These data validate that the SD technology can potentially enhance the storage stability and delivery of nucleic acid-loaded LNPs. Moreover, our findings are also aligned with recent studies where successful SD of mRNA-LNPs was reported using sugar-based drying matrices intended for inhalation delivery [18, 19].

Conclusion

This study presented a comprehensive analysis of the shear stress's impact on LNPs' colloidal stability during the SD process, with a specific focus on tRNA-loaded LNPs. The SD process was optimized for LNPs, while carefully considering the impact of shear stress and thermal stress on their colloidal stability. No correlation was found between the drying temperature and the increase in LNPs'Z-Average and PdI, which may be attributed not only to trehalose's protective effect, but also to factors like evaporative cooling and short residence times. Nevertheless, shear stress impacted colloidal stability of LNPs, particularly for R_{atom} above 4.6. This sensitivity to shear stress might be attributed to the aqueous core of the LNPs, which imparts a more fluid nature compared to SLNs. A drying matrix optimization was performed to counter the shear stress effect during SD and maintain LNPs'colloidal stability. The combination of 10% (w/v) sucrose and 0.1% (w/v) P188 proved to be the most effective stabilizing formulation during SD. P188 demonstrated its ability to protect LNPs against shear stress, possibly by inserting itself within lipid layers. The optimal P188 concentration was found to be slightly below its CMC, preventing the formation of micelles that could destabilize lipid layers.

FD was used as benchmark due to its low shear stress characteristic. In FD, the drying matrix significantly influenced LNPs' protection against processing stresses. When combined with trehalose, P188 improved colloidal stability after FD, demonstrating its ability to stabilize LNPs against various stresses, besides shear stress. Additionally, sucrose limited the increase in Z-Average associated with slow freezing rates, possibly due to sucrose's lower crystallization tendency compared to trehalose. These results highlight the crucial role of the drying matrix in mitigating process-induced stresses on LNPs. Ultimately, the optimized drying matrix and SD process conditions were employed to dry mRNA-loaded LNPs. Spray drying was successfully conducted, validating that SD can be a feasible drying technology for mRNA-LNPs, with the potential to enhance the storage stability and improve the delivery of nucleic acid-loaded LNPs.

Overall, this work sheds light on the importance of both process and formulation optimization to maintain LNPs'colloidal stability during drying and demonstrated that SD can be comparable to gold standard FD as a mild technology, to dry biomolecules, thus advancing the field of LNPs-based therapeutics.

Acknowledgements This work was funded by Hovione Farmaciência S.A. and Fundação para a Ciência e Tecnologia (FCT) through the doctoral fellowship PBID/BDE/11 and SFRH/BD/151219/2021. This work was developed within the scope of the project CICECO-Aveiro Institute of Materials, UIDB/50011/2020 (DOI https://doi.org/10.54499/UIDB/50011/2020), UIDP/50011/2020 (DOI https://doi.org/10.54499/UIDP/50011/2020) & LA/P/0006/2020 (DOI https://doi.org/10.54499/LA/P/0006/2020), financed by national funds through the FCT/MCTES (PIDDAC) and within the scope of the project Associate Laboratory for Green Chemistry, LA/P/0008/2020 (DOI https://doi.org/10.54499/LA/P/0008/2020), UIDP/50006/2020 (DOI https://doi.org/10.54499/UIDP/50006/2020) and UIDB/50006/2020 (DOI https://doi.org/10.54499/UIDB/50006/2020).

Author contributions Susana Farinha and Rute Mota – Performed the experiments, data analysis and contributed to the interpretation of results and manuscript writing.

Carolina Lopes and Ricardo Velez – Conducted some of the experiments and contributed to the interpretation of results.

Mara G. Freire, Ana Aguiar-Ricardo and Miguel Ângelo Rodrigues – Revised the manuscript.

Luís Miguel Marques, Joana S. Cristóvão, Paulo R. Lino – Led the project conception, supervised the research process, reviewed and edited the manuscript.

Data availability Not applicable.

Declarations

Conflict of Interest Authors declare no conflicts on interest.
AI technology was used to assist in improving the text of the manuscript.

References

1. Arabi F, Mansouri V, Ahmadbeigi N. Gene therapy clinical trials, where do we go? An overview. Biomedicine & Pharmacotherapy. 2022;153:113324. Available from: https://linkinghub.elsevier.com/retrieve/pii/S0753332222007132.
2. Lopes C, Cristóvão J, Silvério V, Lino PR, Fonte P. Microfluidic production of mRNA-loaded lipid nanoparticles for vaccine applications. Expert Opin Drug Deliv. 2022;19:1381–96. Available from: https://doi.org/10.1080/17425247.2022.2135502.
3. Lopes C, Cristóvão J, Silvério V, Lino PR, Fonte P. Microfluidic production of mRNA-loaded lipid nanoparticles for vaccine applications. Expert Opin Drug Deliv. 2022;19:1381–96.
4. European Medicines Agency. Assessment report: COVID-19 Vaccine Comirnaty. EMA/707383/2020 Corr1*. 2021;31:1–140. Available from: https://www.ema.europa.eu/en/documents/assessment-report/comirnaty-epar-public-assessment-report_en.pdf.

5. Uddin MN, Roni MA. Challenges of Storage and Stability of mRNA-Based COVID-19 Vaccines. Vaccines (Basel). 2021;9:1033. Available from: https://www.mdpi.com/2076-393X/9/9/1033.
6. Schoenmaker L, Witzigmann D, Kulkarni JA, Verbeke R, Kersten G, Jiskoot W, et al. mRNA-lipid nanoparticle COVID-19 vaccines: Structure and stability. Int J Pharm. 2021;601:120586. Available from: https://doi.org/10.1016/j.ijpharm.2021.120586.
7. Crommelin DJA, Anchordoquy TJ, Volkin DB, Jiskoot W, Mastrobattista E. Addressing the Cold Reality of mRNA Vaccine Stability. J Pharm Sci. 2020;110:997–1001. Available from: https://doi.org/10.1016/j.xphs.2020.12.006.
8. Farinha S, Sá J V., Lino PR, Galésio M, Pires J, Rodrigues MÂ, et al. Spray Freeze Drying of Biologics: A Review and Applications for Inhalation Delivery. Pharm Res. 2023;40:1115–40. Available from: https://link.springer.com/10.1007/s11095-022-03442-4.
9. Daneshmand B, Faghihi H, Amini Pouya M, Aghababaie S, Darabi M, Vatanara A. Application of disaccharides alone and in combination, for the improvement of stability and particle properties of spray-freeze dried IgG. Pharm Dev Technol. 2019;24:439–47.
10. Pouya MA, Daneshmand B, Aghababaie S, Faghihi H, Vatanara A. Spray-Freeze Drying: a Suitable Method for Aerosol Delivery of Antibodies in the Presence of Trehalose and Cyclodextrins. AAPS PharmSciTech. 2018;19:2247–54.
11. Kommineni N, Butreddy A, Sainaga Jyothi VGS, Angsantikul P. Freeze-drying for the preservation of immunoengineering products. iScience. 2022;25:105127.
12. Maltesen MJ, van de Weert M. Drying methods for protein pharmaceuticals. Drug Discov Today Technol. 2008;5:81–8.
13. Muramatsu H, Lam K, Bajusz C, Laczkó D, Karikó K, Schreiner P, et al. Lyophilization provides long-term stability for a lipid nanoparticle-formulated, nucleoside-modified mRNA vaccine. Mol Ther. 2022;30:1–11.
14. Malamatari M, Charisi A, Malamataris S, Kachrimanis K, Nikolakakis I. Spray drying for the preparation of nanoparticle-based drug formulations as dry powders for inhalation. Processes. 2020;8.
15. Sebastião IB, Bhatnagar B, Tchessalov S, Ohtake S, Plitzko M, Luy B, et al. Bulk Dynamic Spray Freeze-Drying Part 2: Model-Based Parametric Study for Spray-Freezing Process Characterization. J Pharm Sci. 2019;108:2075–85.
16. Marschall C, Witt M, Hauptmeier B, Friess W. Powder suspensions in non-aqueous vehicles for delivery of therapeutic proteins. Eur J Pharm Biopharm. 2021;161:37–49.
17. Donthi MR, Butreddy A, Saha RN, Kesharwani P, Dubey SK. Leveraging spray drying technique for advancing biologic product development–A mini review. Health Sciences Review. 2024;10:100142. Available from: https://linkinghub.elsevier.com/retrieve/pii/S2772632023000685.
18. Friis KP, Gracin S, Oag S, Leijon A, Sand E, Lindberg B, et al. Spray dried lipid nanoparticle formulations enable intratracheal delivery of mRNA. Journal of Controlled Release. 2023;363:389–401. Available from: http://www.ncbi.nlm.nih.gov/pubmed/37741463.
19. Sarode A, Patel P, Vargas-Montoya N, Allawzi A, Zhilin-Roth A, Karmakar S, et al. Inhalable dry powder product (DPP) of mRNA lipid nanoparticles (LNPs) for pulmonary delivery. Drug Deliv Transl Res. 2023; Available from: https://doi.org/10.1007/s13346-023-01402-y.
20. Zimmermann CM, Baldassi D, Chan K, Adams NBP, Neumann A, Porras-Gonzalez DL, et al. Spray drying siRNA-lipid nanoparticles for dry powder pulmonary delivery. Journal of Controlled Release. 2022;351:137–50. Available from: https://doi.org/10.1016/j.jconrel.2022.09.021.
21. Zimmermann CM, Deßloch L, Jürgens DC, Luciani P, Merkel OM. Evaluation of the effects of storage conditions on spray-dried siRNA-LNPs before and after subsequent drying. European Journal of Pharmaceutics and Biopharmaceutics. 2023;193:218–26. Available from: https://linkinghub.elsevier.com/retrieve/pii/S0939641123002965.
22. Pinto JT, Faulhammer E, Dieplinger J, Dekner M, Makert C, Nieder M, et al. Progress in spray-drying of protein pharmaceuticals: Literature analysis of trends in formulation and process attributes. Drying Technol. 2021;39:1415–46.
23. Samborska K, Poozesh S, Barańska A, Sobulska M, Jedlińska A, Arpagaus C, et al. Innovations in spray drying process for food and pharma industries. J Food Eng. 2022;321.
24. Mandato S, Rondet E, Delaplace G, Barkouti A, Galet L, Accart P, et al. Liquids' atomization with two different nozzles: Modeling of the effects of some processing and formulation conditions by dimensional analysis. Powder Technol. 2012;224:323–30.
25. Liang W, Chow MYT, Chow SF, Chan HK, Kwok PCL, Lam JKW. Using two-fluid nozzle for spray freeze drying to produce porous powder formulation of naked siRNA for inhalation. Int J Pharm. 2018;552:67–75.
26. Anandharamakrishnan C. Handbook of Drying for Dairy Products. Chichester, UK: John Wiley & Sons, Ltd; 2017.
27. Henriques P, Fortuna A, Doktorovová S. Spray dried powders for nasal delivery: Process and formulation considerations. Eur J Pharm Biopharm. 2022;176:1–20.
28. Begum F, Amin S. Investigating the Influence of Polysorbate 20/80 and Polaxomer P188 on the Surface & Interfacial Properties of Bovine Serum Albumin and Lysozyme. Pharm Res. 2019;36.
29. Schoenmaker L, Witzigmann D, Kulkarni JA, Verbeke R, Kersten G, Jiskoot W, et al. mRNA-lipid nanoparticle COVID-19 vaccines: Structure and stability. Int J Pharm. 2021;601:120586. Available from: https://doi.org/10.1016/j.ijpharm.2021.120586.
30. Mochizuki S, Kanegae N, Nishina K, Kamikawa Y, Koiwai K, Masunaga H, et al. The role of the helper lipid dioleoylphosphatidylethanolamine (DOPE) for DNA transfection cooperating with a cationic lipid bearing ethylenediamine. Biochimica et Biophysica Acta (BBA) - Biomembranes. 2013;1828:412–8.
31. Roces CB, Lou G, Jain N, Abraham S, Thomas A, Halbert GW, et al. Manufacturing Considerations for the Development of Lipid Nanoparticles Using Microfluidics. Pharmaceutics. 2020;12:1095. Available from: https://www.mdpi.com/1999-4923/12/11/1095.
32. Blakney AK, McKay PF, Yus BI, Aldon Y, Shattock RJ. Inside out: optimization of lipid nanoparticle formulations for exterior complexation and in vivo delivery of saRNA. Gene Ther. 2019;26:363–72.
33. Schoenmaker L, Witzigmann D, Kulkarni JA, Verbeke R, Kersten G, Jiskoot W, et al. mRNA-lipid nanoparticle COVID-19 vaccines: Structure and stability. Int J Pharm. 2021;601: 120586.
34. EMA. Onpattro: Summary of Product Characteristics. 2018. Available from: https://www.ema.europa.eu/en/documents/product-information/onpattro-epar-product-information_en.pdf. Cited 2023 Jan 6.
35. Suzuki Y, Hyodo K, Tanaka Y, Ishihara H. SiRNA-lipid nanoparticles with long-term storage stability facilitate potent gene-silencing in vivo. J Control Release. 2015;220:44–50.
36. Chen C, Han D, Cai C, Tang X. An overview of liposome lyophilization and its future potential. J Control Release. 2010;142:299–311.
37. Abdelwahed W, Degobert G, Stainmesse S, Fessi H. Freeze-drying of nanoparticles: Formulation, process and storage considerations. Adv Drug Deliv Rev. 2006;58:1688–713.
38. Franzé S, Selmin F, Samaritani E, Minghetti P, Cilurzo F. Lyophilization of Liposomal Formulations: Still Necessary. Still Challenging Pharmaceutics. 2018;10:139.
39. Crommelin DJA, Anchordoquy TJ, Volkin DB, Jiskoot W, Mastrobattista E. Addressing the Cold Reality of mRNA Vaccine

Stability. J Pharm Sci. 2021;110:997–1001. Available from: https://linkinghub.elsevier.com/retrieve/pii/S0022354920307851.
40. Oude Blenke E, Örnskov E, Schöneich C, Nilsson GA, Volkin DB, Mastrobattista E, et al. The Storage and In-Use Stability of mRNA Vaccines and Therapeutics: Not A Cold Case. J Pharm Sci. 2023;112:386–403. Available from: https://linkinghub.elsevier.com/retrieve/pii/S0022354922005147.
41. Zhao P, Hou X, Yan J, Du S, Xue Y, Li W, et al. Long-term storage of lipid-like nanoparticles for mRNA delivery. Bioact Mater. 2020;5:358–63.
42. Costa C, Nobre B, Matos AS, Silva AS, Casimiro T, Corvo ML, et al. Inhalable hydrophilic molecule-loaded liposomal dry powder formulations using supercritical CO2 – assisted spray-drying. Journal of CO2 Utilization. 2021;53:101709. Available from: https://doi.org/10.1016/j.jcou.2021.101709.
43. An J, Forchheimer D, Sävmarker J, Brülls M, Frenning G. Nanoscale characterization of PEGylated phospholipid coatings formed by spray drying on silica microparticles. J Colloid Interface Sci. 2020;577:92–100.
44. Siew A. Exploring the use of aseptic spray drying in the manufacture of biopharmaceutical injectables. Pharm Technol. 2016;40:24–7.
45. Wang B, Timilsena YP, Blanch E, Adhikari B. Characteristics of bovine lactoferrin powders produced through spray and freeze drying processes. Int J Biol Macromol. 2017;95:985–94.
46. Samaridou E, Heyes J, Lutwyche P. Lipid nanoparticles for nucleic acid delivery: Current perspectives. Adv Drug Deliv Rev. 2020;154–155:37–63.
47. Chavan T, Muttil P, Kunda NK. Introduction to Nanomedicine in Drug Delivery. AAPS Advances in the Pharmaceutical Sciences Series. 2020.
48. Yue-Xing C, Fei-Fei Y, Han W, Tao-Tao F, Chun-Yu L, Li-Hui Q, et al. The effect of l -leucine on the stabilization and inhalability of spray-dried solid lipid nanoparticles for pulmonary drug delivery. J Drug Deliv Sci Technol. 2018;46:474–81.
49. Lball R, Bajaj P, Whitehead KA. Achieving long-term stability of lipid nanoparticles: Examining the effect of pH, temperature, and lyophilization. Int J Nanomedicine. 2017;12:305–15.
50. Zhang W, Wang G, See E, Shaw JP, Baguley BC, Liu J, et al. Post-insertion of poloxamer 188 strengthened liposomal membrane and reduced drug irritancy and in vivo precipitation, superior to PEGylation. J Control Release. 2015;203:161–9.
51. Maskarinec SA, Hannig J, Lee RC, Lee KYC. Direct observation of poloxamer 188 insertion into lipid monolayers. Biophys J. 2002;82:1453–9.
52. Adhikari U, Goliaei A, Tsereteli L, Berkowitz ML. Properties of poloxamer molecules and poloxamer micelles dissolved in water and next to lipid bilayers: Results from computer simulations. J Phys Chem B. 2016;120:5823–30.
53. Trenkenschuh E, Richter M, Heinrich E, Koch M, Fuhrmann G, Friess W. Enhancing the Stabilization Potential of Lyophilization for Extracellular Vesicles. Adv Healthc Mater. 2022;11.
54. Nazari M, Kurdi M, Heerklotz H. Classifying surfactants with respect to their effect on lipid membrane order. Biophys J. 2012;102:498–506.
55. Patel S, Ashwanikumar N, Robinson E, Xia Y, Mihai C, Griffith JP, et al. Naturally-occurring cholesterol analogues in lipid nanoparticles induce polymorphic shape and enhance intracellular delivery of mRNA. Nat Commun. 2020;11:1–13.
56. Adami RC, Seth S, Harvie P, Johns R, Fam R, Fosnaugh K, et al. An amino acid-based amphoteric liposomal delivery system for systemic administration of siRNA. Mol Ther. 2011;19:1141–51.
57. Lokras A, Chakravarty A, Rades T, Christensen D, Franzyk H, Thakur A, et al. Simultaneous quantification of multiple RNA cargos co-loaded into nanoparticle-based delivery systems. Int J Pharm. 2022;626: 122171.
58. Ćirin D, Krstonošić V, Poša M. Properties of poloxamer 407 and polysorbate mixed micelles: Influence of polysorbate hydrophobic chain. J Ind Eng Chem. 2017;47:194–201.
59. Kim B, Hosn RR, Remba T, Yun D, Li N, Abraham W, et al. Optimization of storage conditions for lipid nanoparticle-formulated self-replicating RNA vaccines. J Control Release. 2023;353:241–53.
60. van den Bogaart G, Hermans N, Krasnikov V, de Vries AH, Poolman B. On the Decrease in Lateral Mobility of Phospholipids by Sugars. Biophys J. 2007;92:1598–605.
61. Suk JS, Xu Q, Kim N, Hanes J, Ensign LM. PEGylation as a strategy for improving nanoparticle-based drug and gene delivery. Adv Drug Deliv Rev. 2016;99:28–51. Available from: https://linkinghub.elsevier.com/retrieve/pii/S0169409X15002173.
62. Cheng F, Wang Y, Bai Y, Liang Z, Mao Q, Liu D, et al. Research Advances on the Stability of mRNA Vaccines. Viruses. 2023;15:668. Available from: https://www.mdpi.com/1999-4915/15/3/668.
63. Tenchov R, Sasso JM, Zhou QA. PEGylated Lipid Nanoparticle Formulations: Immunological Safety and Efficiency Perspective. Bioconjug Chem. 2023;34:941–60. Available from: https://pubs.acs.org/doi/10.1021/acs.bioconjchem.3c00174.
64. Fang Y, Xue J, Gao S, Lu A, Yang D, Jiang H, et al. Cleavable PEGylation: a strategy for overcoming the "PEG dilemma" in efficient drug delivery. Drug Deliv. 2017;24:22–32. Available from: https://www.tandfonline.com/doi/full/10.1080/10717544.2017.1388451.
65. Zhang H, Leal J, Soto MR, Smyth HDC, Ghosh D. Aerosolizable Lipid Nanoparticles for Pulmonary Delivery of mRNA through Design of Experiments. Pharmaceutics. 2020;12:1–16. Available from: https://pubmed.ncbi.nlm.nih.gov/33143328/.
66. Lokugamage MP, Vanover D, Beyersdorf J, Hatit MZC, Rotolo L, Echeverri ES, et al. Optimization of lipid nanoparticles for the delivery of nebulized therapeutic mRNA to the lungs. Nat Biomed Eng. 2021;5:1059–68. Available from: https://doi.org/10.1038/s41551-021-00786-x.
67. Scioli Montoto S, Muraca G, Ruiz ME. Solid Lipid Nanoparticles for Drug Delivery: Pharmacological and Biopharmaceutical Aspects. Front Mol Biosci. 2020;7:1–24. Available from: https://www.frontiersin.org/articles/10.3389/fmolb.2020.587997/full.
68. Suzuki Y, Miyazaki T, Muto H, Kubara K, Mukai Y, Watari R, et al. Design and lyophilization of lipid nanoparticles for mRNA vaccine and its robust immune response in mice and nonhuman primates. Mol Ther Nucleic Acids. 2022;30:226–40.
69. Ingvarsson PT, Yang M, Nielsen HMø, Rantanen J, Foged C. Stabilization of liposomes during drying. Expert Opin Drug Deliv. 2011;8:375–88.
70. Guimarães D, Noro J, Silva C, Cavaco-Paulo A, Nogueira E. Protective Effect of Saccharides on Freeze-Dried Liposomes Encapsulating Drugs. Front Bioeng Biotechnol. 2019;7:1–8.
71. Luo W, O'Reilly Beringhs A, Kim R, Zhang W, Patel SM, Bogner RH, et al. Impact of formulation on the quality and stability of freeze-dried nanoparticles. Eur J Pharm Biopharm. 2021;169:256–67.
72. De Paula RT, Silva CL, Santana MHA, Rosada RS, De La Torre LG. Effects of extrusion, lipid concentration and purity on physico-chemical and biological properties of cationic liposomes for gene vaccine applications. J Microencapsul. 2012;29:759–69.
73. Ohtake S, Schebor C, Palecek SP, De Pablo JJ. Phase behavior of freeze-dried phospholipid-cholesterol mixtures stabilized with trehalose. Biochim Biophys Acta Biomembr. 2005;1713:57–64.
74. Starciuc T, Malfait B, Danede F, Paccou L, Guinet Y, Correia NT, et al. Trehalose or Sucrose: Which of the Two Should be Used for Stabilizing Proteins in the Solid State? A Dilemma Investigated by In Situ Micro-Raman and Dielectric Relaxation Spectroscopies During and After Freeze-Drying. J Pharm Sci. 2020;109:496–504.

75. Fan Y, Rigas D, Kim LJ, Chang F-P, Zang N, McKee K, et al. Physicochemical and structural insights into lyophilized mRNA-LNP from lyoprotectant and buffer screenings. Journal of Controlled Release. 2024;373:727–37. Available from: https://linkinghub.elsevier.com/retrieve/pii/S0168365924005078.
76. Alejo T, Toro-Córdova A, Fernández L, Rivero A, Stoian AM, Pérez L, et al. Comprehensive Optimization of a Freeze-Drying Process Achieving Enhanced Long-Term Stability and In Vivo Performance of Lyophilized mRNA-LNPs. Int J Mol Sci. 2024;25:10603. Available from: https://www.mdpi.com/1422-0067/25/19/10603.
77. Ogawa K, Aikawa O, Tagami T, Ito T, Tahara K, Kawakami S, et al. Stable and inhalable powder formulation of mRNA-LNPs using pH-modified spray-freeze drying. Int J Pharm. 2024;665:124632. Available from: https://linkinghub.elsevier.com/retrieve/pii/S0378517324008664.